Journal of Magnetic Resonance **138,** 1–11 (1999)
Article ID jmre.1999.1704, available online at http://www.idealibrary.com on IDEAL®

Lineshape Calculations on Spreadsheet Software

C. Mayer

Institut für Physikalische und Theoretische Chemie, Universität Duisburg, 47048 Duisburg, Germany

E-mail: hi408ma@uni-duisburg.de

Received June 8, 1998; revised December 1, 1998

Spectral lineshapes reflecting slow molecular reorientation are calculated by a simplified numeric approach based on the stochastic Liouville equation. The relevant reorientation process is described by a stationary Markov operator which is, using a finite grid point method, represented by a matrix with a dimension equivalent to the number of orientational sites. A differential equation for the time evolution of the density matrix allows the development of the overall magnetization to be calculated in consecutive time steps. For increased convenience and flexibility, the algorithm can be installed using commercial spreadsheet software on a regular personal computer.

INTRODUCTION

NMR lineshapes and their variations during relaxation experiments provide a rich source of information on molecular reorientation processes. However, it is not always straightforward to obtain motional parameters from spectral data such as lineshapes and relaxation times, especially if the reorientation occurs in the slow motional regime. A variety of computation methods have been developed in order to simulate magnetic resonance data for given motional parameter sets (*1–6*). Most procedures are based on comprehensive motional models including intramolecular reorientations as well as intermolecular and collective processes. These motions can be accounted for either in terms of correlation functions or by applying a finite grid point approximation. Generally, a stationary Markov operator is defined which, being part of the stochastic Liouville equation, describes the motionally induced change of the spin density matrix. Integration of the first derivative of the density matrix elements in order to obtain the spectral lineshape results in a more or less complicated eigenvalue problem (*5, 6*). Lately, a very effective approach for the simulation of spectra has been developed by N. J. Heaton (*7*), which takes account of the motionally induced time dependence of Hamiltonian operators for individual spins. The evolution of the density matrix is then developed in small time steps by calculating successive powers of a propagator matrix. Finally, the spectral lineshape is obtained by Fourier transformation.

Similar to the alternatives mentioned above, the proposed algorithm is based on the stochastic Liouville equation. Its main advantage compared to the method described by Kothe *et al.* (*5, 6*) is the fact that it avoids the solution of the eigenvalue problem and therefore does not include the sophisticated and time-consuming step of matrix diagonalization. In contrast to the procedure outlined by Heaton (*7*), its implementation is simplified since no powers of a given propagator matrix must be calculated.

The algorithm proposed here again introduces finite steps in the time regime. However, in contrast to the method outlined by Heaton, the overall magnetization is segmented into contributions from various "sites" of common angular orientation. Consequently, the individual Hamiltonian operators that enter the calculation are strictly not time dependent (which they are in the case of Heaton's procedure). The development of each orientational contribution is then numerically calculated by introducing short time intervals somewhat equivalent to the dwell time of the actual experiment. The influence of molecular motion on the individual contributions is approximated by consecutive exchange steps representing motional kinetics. The algorithm is described for an $I = \frac{1}{2}$ system in the presence of a chemical shift anisotropy, but may easily be modified to solve other problems.

The resulting numerical method is therefore simple enough to be implemented into regular spreadsheet software as long as the motional model is not too complicated and does not require too many discrete steps in time and angular orientation. Alternatively, a corresponding Fortran or Pascal program version can be applied (Fortran 77 was used by the author). In any case, hardware requirements and computing times are on a low level. The spreadsheet version offers the advantages of a rapid visualization of the result and a very high variability.

1090-7807/99 $30.00

The versatility of the described algorithm is demonstrated based on different motional models under various simulated experimental conditions. Results are shown for a simple two-site jump motion and for isotropic rotational diffusion. The selection of experimental conditions consists of a simple $\pi/2$ pulse and a Hahn echo sequence with variable pulse separation. All examples have been obtained on a regular personal computer with commercial spreadsheet software within less than 20 s per spectrum.

THEORETICAL CONSIDERATIONS

Time Dependence of the Spin Density Matrix

The time-dependent ensemble average magnetization of any spin system can be conveniently described by the spin density matrix $\rho(t)$ (*8, 9*). In the presence of a time-independent Hamiltonian operator and disregarding any other source of relaxation, it develops according to

$$\frac{\partial}{\partial t}\rho(t) = -i/\hbar[\mathbf{H}, \rho(t)]. \qquad [1]$$

The starting condition for such a development may be generated by any pulse sequence; the effect of a simple $\pi/2$ pulse will be discussed in a following section. Generally, the Hamiltonian $\mathbf{H}$ depends on the molecular orientation, marked by a set of Euler angles $\Omega_n = (\Phi_n, \Theta_n, \Psi_n)$, leading to an angular dependence of ρ and $\mathbf{H}$:

$$\frac{\partial}{\partial t}\rho(\Omega_n, t) = -i/\hbar[\mathbf{H}(\Omega_n), \rho(\Omega_n, t)]. \qquad [2]$$

The term $\rho(\Omega_n, t)$ represents the contribution of a given orientation Ω_n to the time-dependent density matrix $\rho(t)$. We now introduce molecular reorientation by assuming a Markov process where $P(\Omega_n, t)$ is the fraction of molecules with the angular orientation Ω_n at time t (*3*). The orientation Ω_n, given by a set of three Euler angles, refers to the orientation of the molecule and therefore of the interaction tensor (e.g., the chemical shift anisotropy) with respect to the magnetic field. For jump motions, the Euler angle sets Ω_n mark the orientations of specific jump sites. For diffusive motions, the reorientation is approximated by a finite number of angular steps in the Euler angle spheres (*5, 6*). In both cases, the motion is characterized by a differential equation involving a set of rate constants $k_{(\Omega n \rightarrow \Omega n')}$:

$$\frac{\partial}{\partial t}\begin{pmatrix} P(\Omega_1, t) \\ P(\Omega_2, t) \\ P(\Omega_3, t) \\ \cdots \end{pmatrix} = \begin{pmatrix} (-k_{(\Omega_1\rightarrow\Omega_2)} - k_{(\Omega_1\rightarrow\Omega_3)}\cdots) & k_{(\Omega_2\rightarrow\Omega_1)} & k_{(\Omega_3\rightarrow\Omega_1)} & \cdots \\ k_{(\Omega_1\rightarrow\Omega_2)} & (-k_{(\Omega_2\rightarrow\Omega_1)} - k_{(\Omega_2\rightarrow\Omega_3)}\cdots) & k_{(\Omega_3\rightarrow\Omega_2)} & \cdots \\ k_{(\Omega_1\rightarrow\Omega_3)} & k_{(\Omega_2\rightarrow\Omega_3)} & (-k_{(\Omega_3\rightarrow\Omega_1)} - k_{(\Omega_3\rightarrow Q_2)}\cdots) & \cdots \\ \cdots & \cdots & \cdots & \cdots \end{pmatrix} \times \begin{pmatrix} P(\Omega_1, t) \\ P(\Omega_2, t) \\ P(\Omega_3, t) \\ \cdots \end{pmatrix} \qquad [3]$$

or

$$\frac{\partial}{\partial t}P(t) = \Gamma P(t). \qquad [4]$$

Correspondingly, a steady state situation is described by

$$\frac{\partial}{\partial t}\begin{pmatrix} P(\Omega_1, t) \\ P(\Omega_2, t) \\ P(\Omega_3, t) \\ \cdots \end{pmatrix} = 0 \quad \text{or} \quad \Gamma\begin{pmatrix} P(\Omega_1, t) \\ P(\Omega_2, t) \\ P(\Omega_3, t) \\ \cdots \end{pmatrix} = 0. \qquad [5]$$

The populations $P(\Omega_n, t)$ in Eq. [5] may therefore be replaced by time-independent equilibrium populations $P(\Omega_n)$. Examples for different motional matrices Γ will follow. Molecular reorientation represents an additional contribution to the time dependence of the density matrix, since any transfer of molecules from orientation Ω_n to $\Omega_{n'}$ within a time interval Δt will transfer a contribution from $\rho(\Omega_n, t)$ toward $\rho(\Omega_{n'}, t + \Delta t)$. The rates of this transfer and therefore their contribution to the time dependence of $\rho(\Omega_n, t)$ are given by the rate constants in Eq. [3]. Equations

[2] and [3] consequently lead to an overall time dependence of the density matrix given by (*3, 8, 11*)

$$\frac{\partial}{\partial t}\rho(\Omega_n, t) = -i/\hbar[\mathbf{H}(\Omega_n), \rho(\Omega_n, t)] + \sum_{n'}\{-k_{(\Omega_n\rightarrow\Omega_{n'})}[\rho(\Omega_n, t) - \rho^{eq}(\Omega_n)] + k_{(\Omega_{n'}\rightarrow\Omega_n)}[\rho(\Omega_{n'}, t) - \rho^{eq}(\Omega_{n'})]\}, \quad [6]$$

where $\rho^{eq}(\Omega_n)$ stands for the equilibrium state of the density matrix for an orientation Ω_n. With Eq. [6], which basically represents the stochastic Liouville equation, the time dependence of the density matrix elements for all orientations Ω is completely described by a set of coupled differential equations.

Time Dependence of the NMR Signal

Similar to the density matrix, the NMR signal $M(t)$ observed in the rotating frame is time dependent and represents the ensemble average of a number, N, of spins in the sample. The contribution $M(\Omega_n, t)$ from molecules situated in a given orientation Ω_n at time t is related to the density matrix by (*8, 9*)

$$M(\Omega_n, t) = \langle M_{x'}(\Omega_n, t)\rangle + i\langle M_{y'}(\Omega_n, t)\rangle = N\gamma\hbar\,\mathrm{Tr}\{\rho(\Omega_n, t)I^+\}, \quad [7]$$

which for a two-level-system with $I = \frac{1}{2}$ results in (*9*)

$$M(\Omega_n, t) = N\gamma\hbar\rho_{12}(\Omega_n, t) \quad [8]$$

or

$$\frac{\partial}{\partial t}M(\Omega_n, t) = N\gamma\hbar\,\frac{\partial}{\partial t}\rho_{12}(\Omega_n, t). \quad [9]$$

The following description will be restricted to a two-level system. Principally, the procedure may be applied to systems with $I > \frac{1}{2}$ in an analogue manner.

According to Eq. [9], the time dependence for the NMR signal in the presence of molecular motion is obtained from Eq. [6] by multiplication with the factor $(N\gamma\hbar)$:

$$\frac{\partial}{\partial t}M(\Omega_n, t) = -iN\gamma[\mathbf{H}(\Omega_n), \rho(\Omega_n, t)]_{12} + N\gamma\hbar\sum_{n'}\{-k_{(\Omega_n\rightarrow\Omega_{n'})}[\rho_{12}(\Omega_n, t) - \rho_{12}^{eq}(\Omega_n)] + k_{(\Omega_{n'}\rightarrow\Omega_n)}[\rho_{12}(\Omega_{n'}, t) - \rho_{12}^{eq}(\Omega_{n'})]\},$$

or, with

$$N\gamma\hbar\rho_{12}(\Omega_n, t) = M(\Omega_n, t) \quad \text{and} \quad \rho_{12}^{eq}(\Omega_n) = 0,$$

$$\frac{\partial}{\partial t}M(\Omega_n, t) = -iN\gamma[\mathbf{H}(\Omega_n), \rho(\Omega_n, t)]_{12} + \sum_{n'}\{-k_{(\Omega_n\rightarrow\Omega_{n'})}[M(\Omega_n, t)] + k_{(\Omega_{n'}\rightarrow\Omega_n)}[M(\Omega_{n'}, t)]\}. \quad [10]$$

The condition $\rho_{12}^{eq}(\Omega_n) = 0$ is justified since all off-diagonal elements of the spin density matrix vanish in the equilibrium state (*9*).

If we consider a finite step in time Δt, the overall evolution of the signal contribution $\Delta M(\Omega_n, t)$ in the course of Δt is given by the integral of Eq. [10]. In order to numerically solve this integral, an assumption has to be made which is only valid for small time intervals Δt. The processes that occur within the time interval Δt are now approximated by two separate "events":

(1) In the course of the time interval between t and $t + \Delta t$, motional exchange is completely absent. Therefore, all rate constants k are zero and Eq. [10] reduces to

$$\frac{\partial}{\partial t}M(\Omega_n, t) = -iN\gamma[\mathbf{H}(\Omega_n), \rho(\Omega_n, t)]_{12}, \quad [11]$$

which has the general solution represented by a precession in the rotating frame (*9*)

$$M(\Omega_n, t) = M(\Omega_n, 0)\exp[i\omega(\Omega_n)t], \quad [12]$$

where $\omega(\Omega_n)$ is the orientation-dependent offset to the Larmor frequency. The magnetization $M(\Omega_n, t + \Delta t)'$ after this first event therefore becomes

$$M(\Omega_n, t + \Delta t)' = M(\Omega_n, t)\exp[i\omega(\Omega_n)\Delta t]. \quad [13]$$

(2) At the end of the time interval (at $t + \Delta t$), a discontinuous jump motion is assumed, with the jump rate representing the effect of the diffusive motion in the course of Δt. This occurs instantaneously, therefore no precession of the magnetization will be observed during this event. Consequently, Eq. [10] simplifies to

$$\frac{\partial}{\partial t}M(\Omega_n, t) = \sum_{n'}\{-k_{(\Omega_n\rightarrow\Omega_{n'})}[M(\Omega_n, t)] + k_{(\Omega_{n'}\rightarrow\Omega_n)}[M(\Omega_{n'}, t)]\}. \quad [14]$$

The variation of $M(\Omega_n, t + \Delta t)'$ due to this jump motion is then given by

$$M(\Omega_n, t + \Delta t) = M(\Omega_n, t + \Delta t)' + \sum_{n'} \{-k_{(\Omega_n \to \Omega_{n'})}\Delta t[M(\Omega_n, t + \Delta t)'] + k_{(\Omega_{n'} \to \Omega_n)}\Delta t[M(\Omega_{n'}, t + \Delta t)']\}. \quad [15]$$

From now on, a diffusive reorientation of the molecule is approximated by a series of consecutive jump motions. Therefore, it becomes very important to keep Δt sufficiently short in order to avoid artifacts. Although Δt represents an equivalent to the experimental dwell time, it may have to be chosen much smaller in order to correctly describe the effect of the motion. In any case, the result of the calculation should be verified by checking the convergence of the lineshapes with decreasing length of the time interval Δt.

With this approximation, the overall variation of all magnetization contributions is obtained by combining Eqs. [13] and [15]:

$$M(\Omega_n, t + \Delta t) = M(\Omega_n, t)\exp[i\omega(\Omega_n)\Delta t] + \sum_{n'} \{-k_{(\Omega_n \to \Omega_{n'})}\Delta t M(\Omega_n, t)\exp[i\omega(\Omega_n)\Delta t] + k_{(\Omega_{n'} \to \Omega_n)}\Delta t M(\Omega_{n'}, t)\exp[i\omega(\Omega_{n'})\Delta t]\}. \quad [16]$$

Based on this equation and a given starting condition $M(\Omega_n, 0)$, it is now straightforward to numerically calculate time-dependent signal contributions for each angular site Ω_n. Each single value $M(\Omega_n, t + \Delta t)$ is computed from $M(\Omega_n, t)$ and a set of values $M(\Omega_{n'}, t)$ for various $\Omega_{n'}$, depending on the characteristics of the motion. In the spreadsheet implementation of the algorithm, $M(\Omega_n, t)$ is split into real and imaginary contributions which are developed in columns along a given time axis t with a step width Δt:

$$\begin{array}{cccc} 0 & M(\Omega_1, 0)_{\text{real}} & M(\Omega_2, 0)_{\text{real}} & \cdots \\ \Delta t & M(\Omega_1, \Delta t)_{\text{real}} & M(\Omega_2, \Delta t)_{\text{real}} & \cdots \\ 2\Delta t & M(\Omega_1, 2\Delta t)_{\text{real}} & M(\Omega_2, 2\Delta t)_{\text{real}} & \cdots \\ 3\Delta t & M(\Omega_1, 3\Delta t)_{\text{real}} & M(\Omega_2, 3\Delta t)_{\text{real}} & \cdots \\ \cdots & \cdots & \cdots & \cdots \\ t & M(\Omega_1, t)_{\text{real}} & M(\Omega_2, t)_{\text{real}} & \cdots \end{array}$$

$$\times \begin{array}{ccc} M(\Omega_1, 0)_{\text{imag}} & M(\Omega_2, 0)_{\text{imag}} & \cdots \\ M(\Omega_1, \Delta t)_{\text{imag}} & M(\Omega_2, \Delta t)_{\text{imag}} & \cdots \\ M(\Omega_1, 2\Delta t)_{\text{imag}} & M(\Omega_2, 2\Delta t)_{\text{imag}} & \cdots \\ M(\Omega_1, 3\Delta t)_{\text{imag}} & M(\Omega_2, 3\Delta t)_{\text{imag}} & \cdots \\ \cdots & \cdots & \cdots \\ M(\Omega_1, t)_{\text{imag}} & M(\Omega_2, t)_{\text{imag}} & \cdots \end{array}$$

The overall signal amplitudes $M_{\text{tot}}(t)$, actually corresponding to single points in a free induction decay, are easily formed according to

$$M_{\text{tot}}(t) = \sum_n M(\Omega_n, t). \quad [17]$$

The number of actual values for $M(\Omega_n, t)$ created in a complete lineshape calculation is given by the amount of discrete orientations multiplied by the number of time intervals. The computer storage requirements therefore grow considerably with the complexity of the motional model if all values are saved. However, for computation of an overall signal $M_{\text{tot}}(t + \Delta t)$, it is only necessary to have a complete set of $M(\Omega_n, t + \Delta t)$ and $M(\Omega_n, t)$ available; all other values can be overwritten. This is easily done in a Fortran or Pascal version of the algorithm, which allows us to calculate, for example, a problem with 25,000 time intervals and 100,000 discrete orientations on a personal computer. The corresponding spreadsheet setup preserves all values and therefore is limited to 2000 time steps and 99 orientational sites, equivalent to a data volume of 18 MB. On the other hand, it offers significant advantages in terms of versatility and convenience. It includes a simple Fourier transform routine creating a frequency spectrum $f(\omega)$ from the overall FID $M_{\text{tot}}(t)$ according to

$$f(\omega) = \int_{-\infty}^{\infty} M(t)\exp(i\omega t)dt. \quad [18]$$

The spectrum, normalized to a standard area, is displayed next to the FID within approximately 5 s after signal computation. An additional speedup may be realized by applying a fast Fourier transform algorithm.

Starting Condition and the Effect of Pulses

As mentioned in the previous section, the iterative computation of the signal contributions $M(\Omega_n, t)$ is initiated by a given starting value $M(\Omega_n, 0)$. Assuming that a single RF pulse is applied to the system, this starting condition depends on frequency, phase, and duration of the first pulse. The following FID is calculated according to Eqs. [16] and [17]. At any point of time during the simulated evolution of the FID, it is possible to reproduce the effect of additional pulses by a corresponding variation of the signal contributions $M(\Omega_n, t)$.

In general, the consequence of the pulse at time t is calculated from the density matrix before the pulse by a corresponding unitary transformation,

$$\rho(t + \Delta t) = D(\varphi, \vartheta, -\varphi)\rho(t - \Delta t)D^{*-1}(\varphi, \vartheta, -\varphi), \quad [19]$$

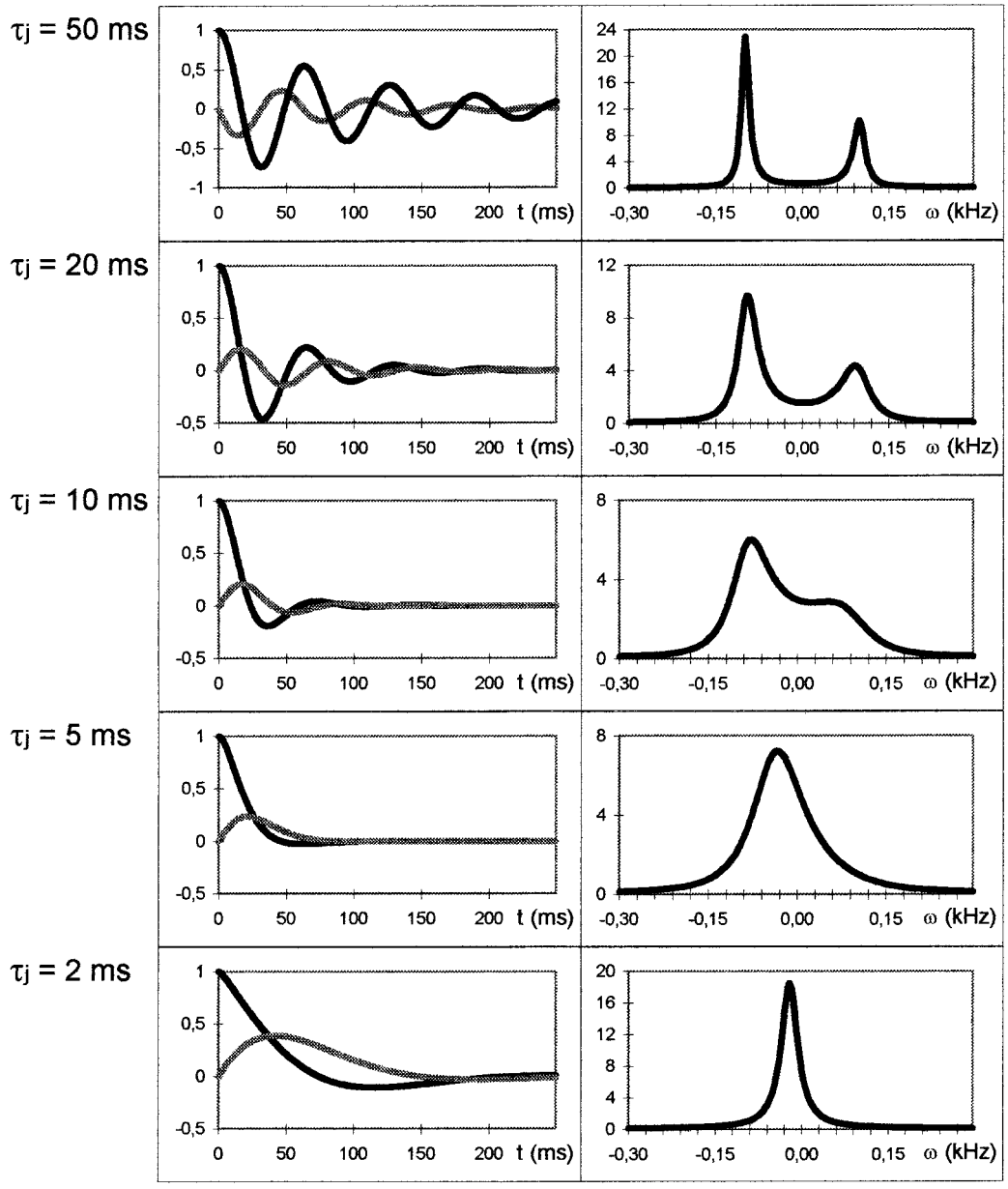

FIG. 1. Calculated free induction decays (left column) and corresponding spectral lineshapes (right column) for a two-site jump motion with correlation times τ_j between 2 and 50 ms. Real parts of the free induction decays (black lines) are normalized to a starting intensity of 1; imaginary parts (gray lines) start at zero intensity. All spectra are normalized to a standard overall area. The simulated experimental condition is a $\pi/2$ pulse in the presence of a jump motion between two sites Ω_1 and Ω_2 with corresponding Larmor frequencies $\omega(\Omega_1) = \omega_0 - 100$ 1/s and $\omega(\Omega_2) = \omega_0 + 100$ 1/s and equilibrium populations $P(\Omega_1) = 0.6$ and $P(\Omega_2) = 0.4$. More simulation parameters are given in the text.

where D is a Wigner rotation matrix with the Hermitian adjoint D^{*-1}, φ is the phase of the pulse, and ϑ is its rotation angle (*6*). In this approximation, the pulse is assumed to be of an infinitesimally short length.

Generally, this procedure must be introduced at the beginning of the simulation, starting with the density matrix for thermal equilibrium, and at each point of the FID calculation where additional pulses occur. In many relevant cases, it is very straightforward to estimate the consequence of a pulse. This may be shown by a simple example: If a $\pi/2$ pulse of infinitesimally short length and phase $-y$ acts on a system in thermal equilibrium, the result, detected in phase x, is given by the steady state population in Ω_n according to

$$M(\Omega_n, 0) \propto P(\Omega_n). \qquad [20]$$

Consequently, all signal contributions start with a real value at time zero. An additional π pulse of phase x after a time period τ leads to an inversion of the imaginary part of $M(\Omega_n, t)$. Such a combination would result, in nature as well as in the corresponding computation, in the well-known formation of a Hahn echo.

It must be mentioned that with the simple procedure described above, the description of RF pulses is restricted to pulses which create magnetization in the xy plane only. Therefore, it is limited to an initial $\pi/2$ pulse followed by one or more π pulses. For all other conditions, it would be necessary to develop the complete density matrix instead of only its element ρ_{12}, which is principally doable but would significantly complicate the problem.

REPRESENTATIVE RESULTS

Two-Site Jump Motion

The simplest case of a molecular reorientation process influencing spectral lineshape is a jump motion between two orientations Ω_1 and Ω_2. Its effect depends on the difference between two corresponding Hamiltonians, $\mathbf{H}(\Omega_1)$ and $\mathbf{H}(\Omega_2)$, and Larmor frequencies, $\omega(\Omega_1)$ and $\omega(\Omega_2)$. The rate of the motion is characterized by an average residence time τ_j, the equilibrium populations of site 1 and 2 by $P(\Omega_1)$ and $P(\Omega_1)$, respectively. In this simple case, the relevant Markov operator is represented by a matrix with four elements k_{nm}. It must fulfill the requirement of Eq. [4],

$$\begin{pmatrix} -k_{(\Omega_1\to\Omega_2)} & k_{(\Omega_2\to\Omega_1)} \\ k_{(\Omega_1\to\Omega_2)} & -k_{(\Omega_2\to\Omega_1)} \end{pmatrix} \begin{pmatrix} P(\Omega_1) \\ P(\Omega_2) \end{pmatrix} = 0. \qquad [21]$$

With τ_j as the average residence time, the matrix elements of Γ are given by

$$k_{(\Omega_2\to\Omega_1)} = P(\Omega_1)/\tau_j \qquad [22a]$$

$$k_{(\Omega_1\to\Omega_2)} = P(\Omega_2)/\tau_j. \qquad [22b]$$

Based on these data, the development of the FID signal can be calculated using Eqs. [16] and [17], if the starting conditions are defined. Figure 1 shows a representative set of calculated FIDs (only an initial section of each FID is shown) and spectra resulting from a $\pi/2$-pulse experiment. The average residence time τ_j is varied between 50 and 2 ms while the equilibrium populations are given by $P(\Omega_1) = 0.6$ and $P(\Omega_2) = 0.4$. These parameters given, Eqs. [22a] and [22b] allow the calculation of the rate constants $k_{(\Omega_2\to\Omega_1)}$ and $k_{(\Omega_1\to\Omega_2)}$. The two jump sites, Ω_1 and Ω_2, are assigned to two different Larmor frequencies, $\omega(\Omega_1) = \omega_0 - 100$ 1/s and $\omega(\Omega_2) = \omega_0 + 100$ 1/s. The time axis is segmented into 2000 time intervals Δt of 0.5 ms duration. With these data and the initial condition defined by Eq. [20], FIDs and spectra shown in Fig. 1 were obtained within 5 s on a spreadsheet. The spin–spin relaxation time for each data set corresponds to the observable length of the FID; in the case shown, a minimum is observed near $\tau_j = 5$ ms which corresponds to $1/\Delta\omega$.

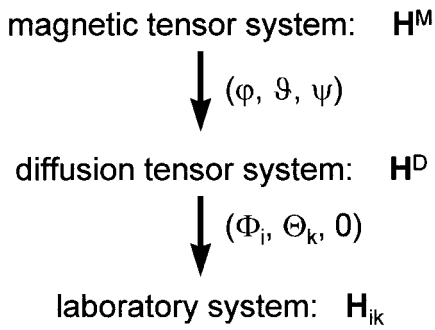

FIG. 2. Notation for coordinate systems and Euler angles required for a description of a rotational diffusion.

Isotropic and Anisotropic Rotational Diffusion

A rotational diffusion in a three-dimensional space is characterized by time-dependent Euler angles Φ, Θ, and Ψ describing the transformation from the diffusion tensor system to the laboratory system (Fig. 2). Due to the symmetry of the experimental setup, the Hamiltonian operator is invariant against Ψ, so this angle is not taken into account in the further evaluation.

In the grid point approximation, the complete sphere of possible Euler angles is then segmented into a finite number of sites, Ω_n, defined by Φ_i and Θ_k, such that every index n now corresponds to one set of indices k and i. The equilibrium population of the site $\Omega_n = \Omega_{ik} = (\Phi_i, \Theta_k)$ is given by P_{ik}. The Euler angles Φ_i and Θ_k are chosen according to

$$0 \le \Phi_i \le 2\pi \qquad [23a]$$

$$0 \le \Theta_k \le \pi, \qquad [23b]$$

with

$$i = 1, 2, \ldots, N_\Phi \quad \text{and} \quad k = 1, 2, \ldots, N_\Theta,$$

in such a way that angular steps $\Delta\Phi$ and $\Delta\Theta$ between neighboring sites are always identical. The matrix for the corresponding Markov process has an overall dimension depending on the site numbers N_Φ and N_Θ. Based on the idea of rotational diffusion (*13, 14*), their elements $k_{ii'kk} = k_{(\Phi i\to\Phi i')}$ and $k_{iikk'} = k_{(\Theta k\to\Theta k')}$ must fulfill the equations (*5, 6, 11*)

$$k_{i(i+1)kk} + k_{i(i-1)kk} = N_\Phi^2/(12\pi^2\tau_\parallel) \qquad [24a]$$

$$k_{i(i+1)kk}P_{ik} = k_{(i+1)ikk}P_{(i+1)k} \qquad [24b]$$

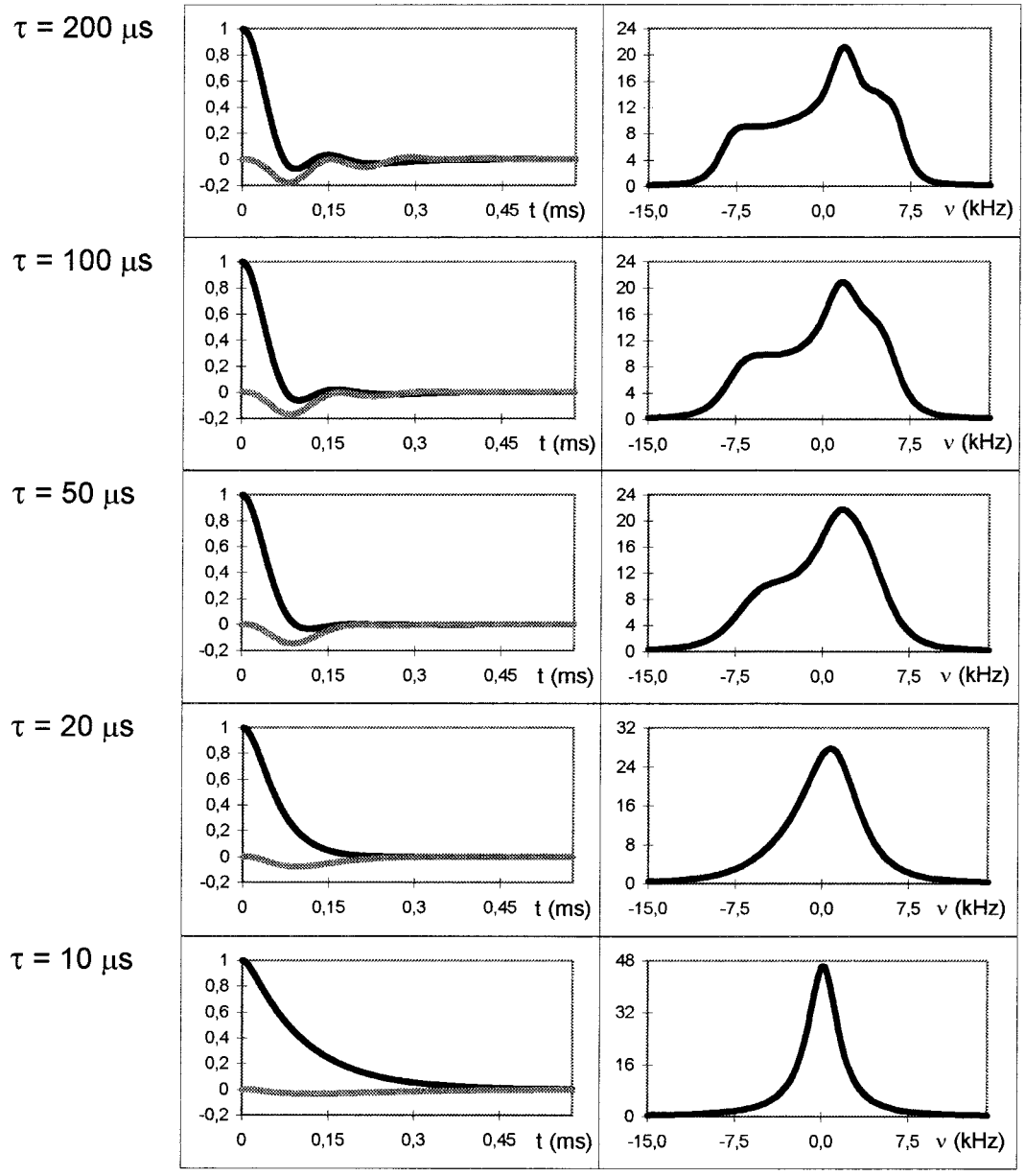

FIG. 3. Calculated free induction decays (left column) and corresponding spectral lineshapes (right column) for an isotropic rotational diffusion with correlation times $\tau = \tau_\perp = \tau_\parallel$ between 10 and 200 μs. Real parts of the free induction decays (black lines) are normalized to a starting intensity of 1; imaginary parts (gray lines) start at zero intensity. All spectra are normalized to a standard overall area. The simulated experimental condition is represented by an initial $\pi/2$ pulse. The interaction is assumed to be a chemical shift anisotropy with tensor elements $S_{11}/S_{22}/S_{33}$ = 2 kHz/8 kHz/−10 kHz; more details are given in the text.

and

$$k_{iik(k+1)} + k_{iik(k-1)} = N_\Theta^2/(3\pi^2\tau_\perp) \qquad [25a]$$

$$k_{iik(k+1)}P_{ik} = k_{ii(k+1)k}P_{i(k+1)}. \qquad [25b]$$

The diagonal elements of the matrix are derived from the requirements of a stationary process given by Eq. [4]:

$$k_{iikk} = -k_{i(i+1)kk} - k_{i(i-1)kk} - k_{iik(k+1)} - k_{iik(k-1)}. \qquad [26]$$

All other matrix elements, except for $k_{(N\Phi)1\,kk}$ and $k_{1(N\Phi)\,kk}$, which characterize the transfer between the first and the last sites in Φ according to Eqs. [24a] and [24b], are zero. The correlation times $\tau_\parallel$ and $\tau_\perp$ describe the reorientation around axes parallel or vertical to the symmetry axis of the diffusion tensor, respectively (*6*, *13*, *14*). The anisotropy of the motion depends on the ratio of both values. For an isotropic motion, $\tau_\parallel$ and $\tau_\perp$ are identical.

Without an orienting potential, the equilibrium population

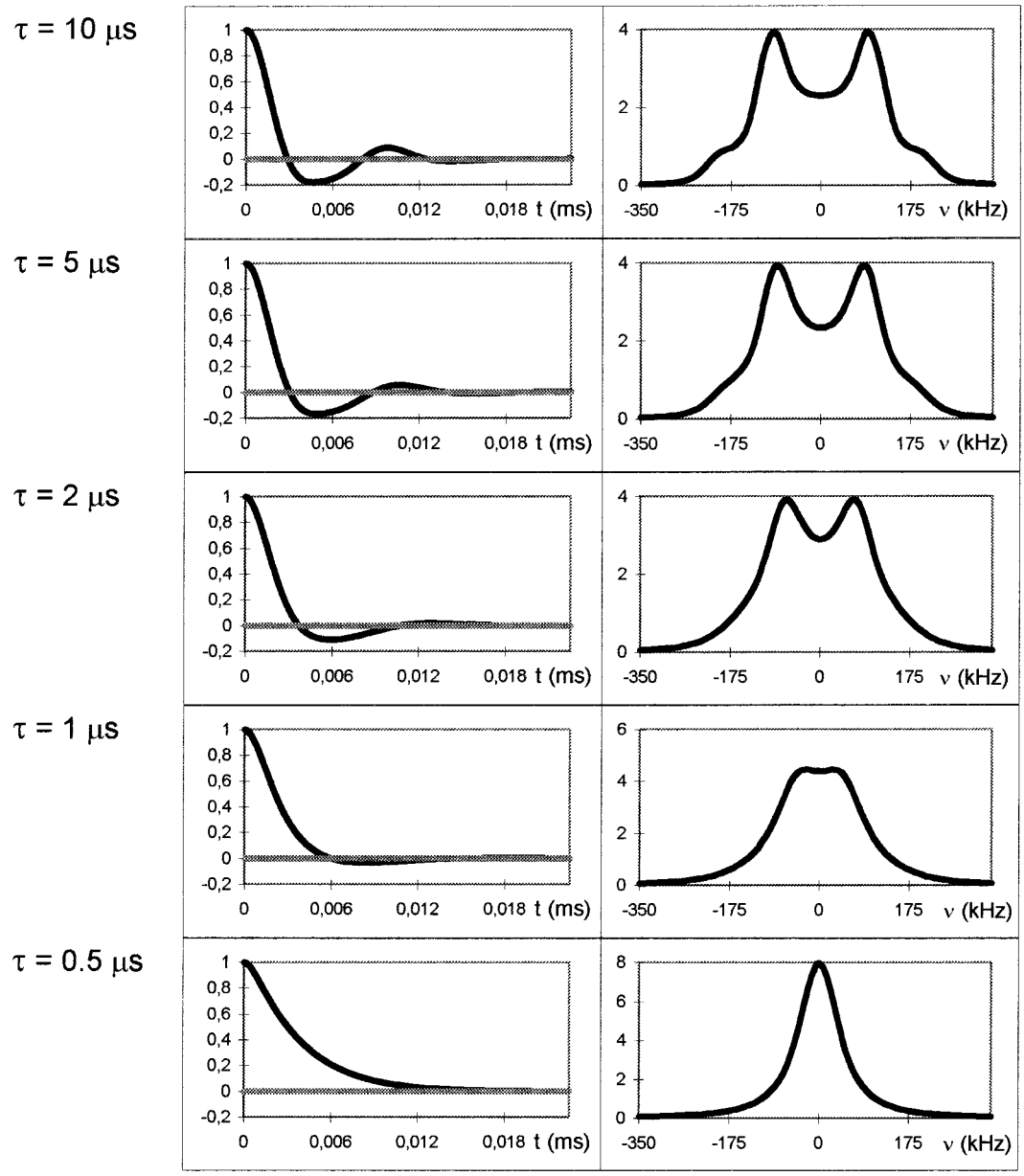

FIG. 4. Calculated free induction decays (left column) and corresponding spectral lineshapes (right column) for an isotropic rotational diffusion with correlation times $\tau = \tau_\perp = \tau_\parallel$ between 0.5 and 10 μs. Real parts of the free induction decays (black lines) are normalized to a starting intensity of 1; imaginary parts (gray lines) start and remain at zero intensity. All spectra are normalized to a standard overall area. The simulated experimental condition is represented by an initial $\pi/2$ pulse. The interaction is assumed to be a quadrupolar coupling represented by tensor elements $Q_{11}/Q_{22}/Q_{33}$ = 100 kHz/150 kHz/−250 kHz; other parameters are identical to those for Fig. 3.

P_{ik} of any site $\Omega_n = (\Phi_i, \Theta_k)$ with the Euler angle Θ_k is given by

$$P_{ik} = \frac{\sin \Theta_k}{N_\Phi \sum_{k'=1}^{N_\Theta} \sin \Theta_{k'}}. \qquad [27]$$

In the presence of an orienting potential of any kind, Eq. [27] must be replaced by a suitable orientational distribution function (*6*).

Finally, the Hamiltonian operators $\mathbf{H}_{ik}$ corresponding to all sites in Φ and Θ must be calculated by two coordinate transformations according to Fig. 2 (*6*): First, the Hamiltonian $\mathbf{H}^{\mathrm{M}}$ is transformed from the magnetic tensor system (where its

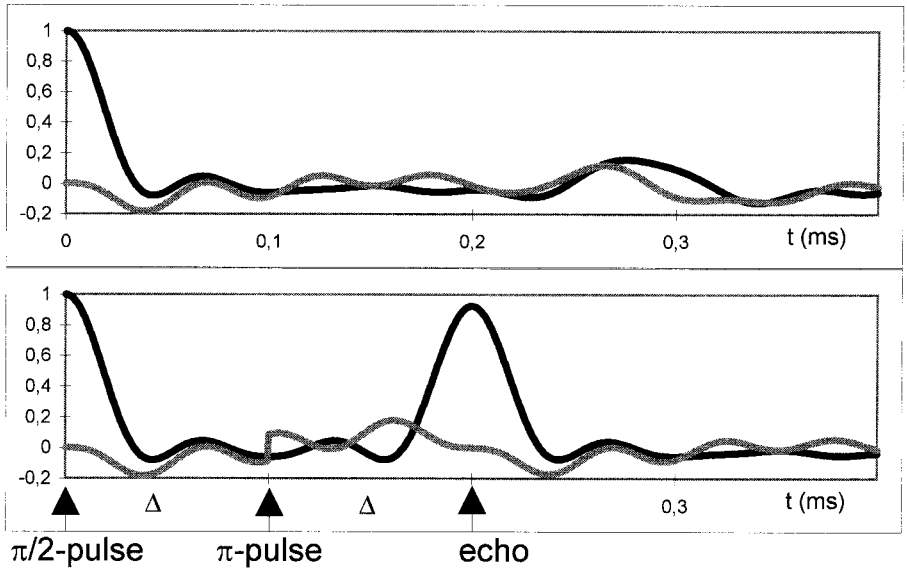

FIG. 5. Effect of an additional π pulse on the development of a characteristic NMR signal (bottom) compared with the original free induction decay (top). In the case shown, the π pulse after a waiting period Δ inverts the imaginary part of the free induction decay (bottom, gray line) while the real part initially remains unaffected. This leads to the formation of a Hahn echo signal after another waiting period Δ. The example shown refers to a slow ($\tau = 100$ ms) rotational diffusion of the tensor given in Fig. 3.

off-diagonal matrix elements are zero) to the molecular diffusion tensor system using a set of fixed Euler angles (φ, ϑ, ψ), which basically describes the orientation of the interaction tensor with respect to the rotation axis of the molecule. Such a transformation is represented by an Euler rotation matrix $\mathbf{T}(\varphi, \vartheta, \psi)$ according to

$$\mathbf{H}^{\mathrm{D}} = \mathbf{T}(\varphi, \vartheta, \psi)\mathbf{H}^{\mathrm{M}}\mathbf{T}^{-1}(\varphi, \vartheta, \psi). \qquad [28]$$

A second transformation, based on the Euler angles Φ_i and Θ_k, which describe the orientation of molecules in a site Ω_{ik} with respect to the magnetic field, leads from the diffusion tensor system to the laboratory system (Fig. 2):

$$\mathbf{H}_{\mathbf{ik}} = \mathbf{T}(\Phi_i, \Theta_k, 0)\mathbf{H}^{\mathrm{D}}\mathbf{T}^{-1}(\Phi_i, \Theta_k, 0). \qquad [29]$$

In the case of an isotropic motion, a defined rotation axis of the molecule does not exist and the result becomes independent from φ, ϑ, and ψ (which therefore may be set to zero, as has been done for the following examples).

Figure 3 shows FIDs (left column: real part, black; imaginary part, gray) and spectra (right column) resulting from the described algorithm. Again, they correspond to a simple $\pi/2$-pulse experiment. In these cases, $\tau_\perp$ is identical to $\tau_\parallel$, characterizing the motion as an isotropic rotational diffusion. The frequencies $\omega(\Omega_{ik})$ are derived from a chemical shift anisotropy tensor S^{M} with tensor elements $S_{11}/S_{22}/S_{33} = 2$ kHz/8 kHz/-10 kHz by the transformation described above (with $\varphi = \vartheta = \psi = 0$). With $N_\Phi = 9$ and $N_\Theta = 11$, the diffusive motion is approximated by a set of 99 discrete orientations. The correlation time $\tau = \tau_\parallel = \tau_\perp$ is varied between 10 and 200 μs. The FIDs are simulated over 2000 time intervals of 0.6-μs duration; their initial section is shown in Fig. 3. Together with a corresponding spectrum, each FID is obtained within 15 s on a personal computer.

Figure 4 refers to spectral results from a quadrupolar interaction tensor as in the case of a ^{2}H NMR experiment. The corresponding quadrupolar coupling tensor is represented by tensor elements $Q_{11}/Q_{22}/Q_{33} = 100$ kHz/150 kHz/-250 kHz. The correlation time $\tau = \tau_\perp = \tau_\parallel$ for the isotropic diffusive motion is varied between 0.5 and 10 μs and again approximated by 99 discrete orientations. Initial sections of the FIDs, which have been developed in 2000 steps of 15 ns, are shown in Fig. 4 together with corresponding spectra.

In Fig. 5, the effect of an additional π pulse after a waiting period Δ is shown (bottom) in comparison to the original FID (top). A very slow motion ($\tau = \tau_\perp = \tau_\parallel = 100$ ms) is assumed to suppress the effect of the reorientation for this example. The experiment again starts with an initial $\pi/2$ pulse. After a duration Δ, the imaginary part of the NMR signal (gray line) is inverted by a π pulse which is phase shifted by 90° with respect to the $\pi/2$ pulse. The consequence of this event is the formation of a Hahn echo after another time period Δ ($t = 0.2$ ms in Fig. 5, bottom). Except for its intensity, the following part of the FID is almost identical to the initial part after the $\pi/2$ pulse.

Examples for FIDs and lineshapes resulting from a simulated Hahn echo sequence in the presence of motion are presented in Fig. 6. All parameters, except for the presence of the

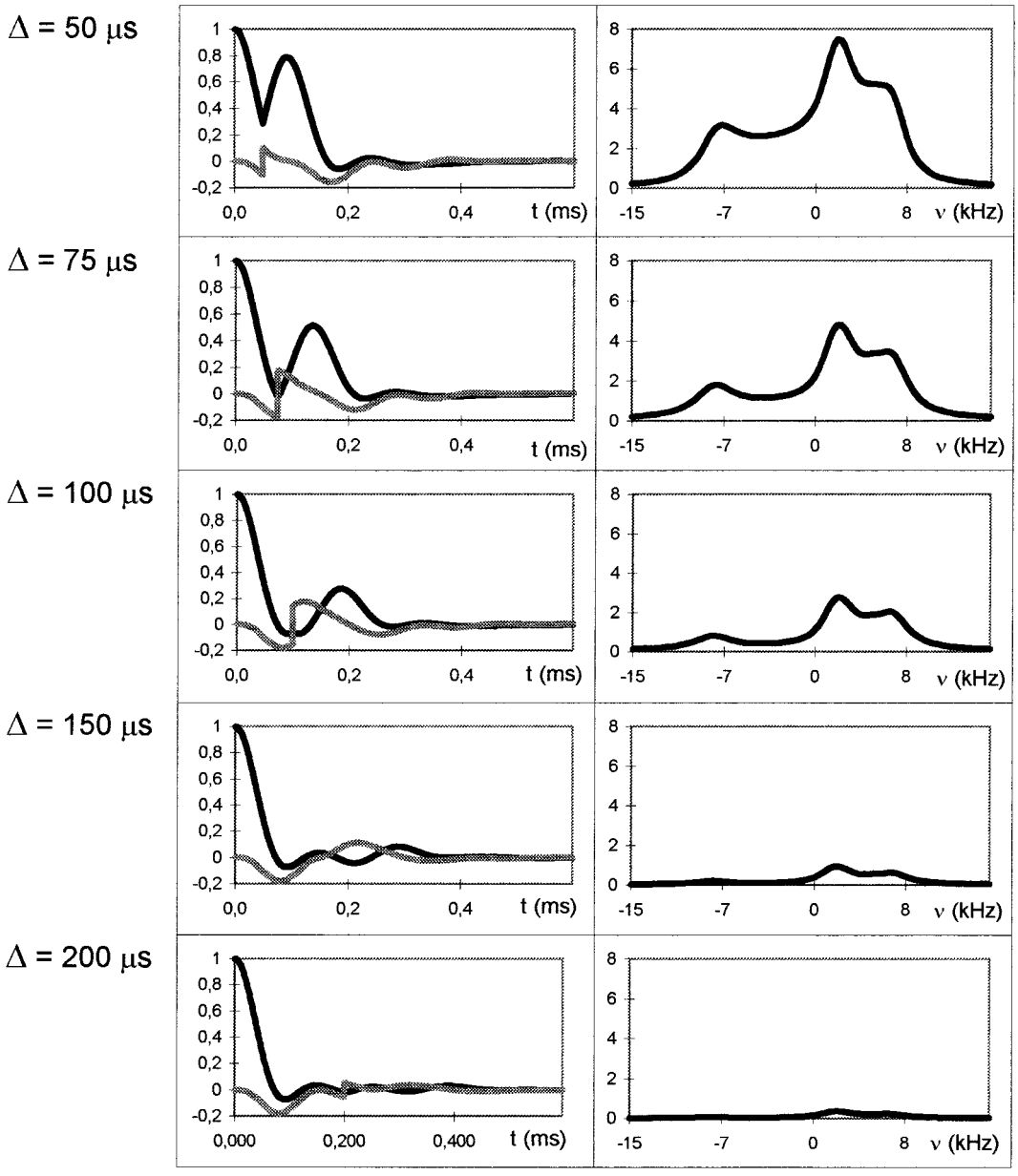

FIG. 6. Calculated free induction decays (left column) and corresponding spectral lineshapes (right column) resulting from a simulated Hahn echo experiment with pulse separations Δ varying between 50 and 200 μs. Lineshapes are obtained by Fourier transformation of the FIDs starting at $t = 2\Delta$. The dependence of the echo signal intensity (and the area of the corresponding spectrum) on the pulse spacing reflects the spin–spin relaxation time T_{2E}.

second pulse, are identical to those for Fig. 3 at 200 μs. The delay between the two pulses is varied from 50 to 200 μs. The echo FID, beginning with the position of the theoretical echo maximum (at $t = 2\Delta$), is submitted to Fourier transformation according to Eq. [18]. The dependence of the echo signal intensity (and the area of the corresponding spectrum) on the pulse spacing reflects the spin–spin relaxation time T_{2E} (*6*).

Parameters such as site numbers, length of the time interval, or the overall number of time intervals must be chosen according to the given conditions. Generally, rapid diffusive motions require fewer sites than slow ones. In the case of a diffusive motion, the length of the time interval Δt should be, as a rule of thumb, at least an order of magnitude smaller than the correlation time of the motion. In the case of extremely rapid reorientations with correlation times near $1/\omega_0$, it is advisable to apply the Redfield approximation based on the described motional model (*15*). Finally, the overall number of sites in the time regime should be sufficient to describe the complete decay of the signal, otherwise artifacts like "wiggles" are observed in the spectral lineshape. In careful studies, all results should be

checked for convergence with increasing site numbers in time and angular orientations.

The finite grid point approximation further allows us to combine rotational diffusion with a jump motion, as is proposed in detail by Kothe *et al.* (*6*). An extension of the technique to a description of experiments under sample spinning conditions is in preparation.

Standard spreadsheet implementations in Microsoft Excel will be transferred by E-mail upon request.

CONCLUSION

In comparison to methods described earlier, the procedure outlined here offers a significantly simplified numeric approach to simulate spectral lineshapes. Despite some limitations due to the additional finite grid point approximation in the time regime, it allows us to approach a very large variety of motional and experimental conditions. In addition, its low-level software and hardware requirements make it suitable for almost any given computer equipment.

ACKNOWLEDGMENT

I thank Wiebren S. Veeman for his general support and helpful comments on the paper.

REFERENCES

1. J. R. Norris and S. I. Weissman, *J. Phys. Chem.* **73,** 3119 (1969).
2. H. Sillescu, *J. Chem. Phys.* **54,** 2110 (1971).
3. J. H. Freed, G. V. Bruno, and C. F. Polnaszek, *J. Phys. Chem.* **75,** 3385 (1971).
4. J. H. Freed, *J. Chem. Phys.* **66,** 4183 (1977).
5. G. Kothe, K.-H. Wassmer, A. Naujok, E. Ohmes, J. Rieser, and K. Wallenfels, *J. Magn. Reson.* **36,** 425 (1979).
6. P. Meier, E. Ohmes, and G. Kothe, *J. Chem. Phys.* **85,** 3598 (1986).
7. N. J. Heaton, *Chem. Phys. Lett.* **252,** 77 (1996).
8. A. Abragam, "The Principles of Nuclear Magnetism," Oxford Univ. Press, London (1961).
9. C. P. Slichter, "Principles of Magnetic Resonance," Springer, Berlin (1978).
10. G. L. Hoatson and K. J. Packer, *Mol. Phys.* **40,** 1153 (1980).
11. G. Kothe, *Mol. Phys.* **33,** 147 (1977).
12. R. Kubo, *in* "Stochastic Processes in Chemical Physics, Advances in Chemical Physics" (K. Shuler, Ed.), Vol. 16, p. 101, Wiley, New York (1969).
13. F. Perrin, *J. Phys. Radium* **5,** 497 (1934).
14. F. Perrin, *J. Phys. Radium* **7,** 1 (1936).
15. C. Mayer, G. Gröbner, K. Müller, K. Weisz, and G. Kothe, *Chem. Phys. Lett.* **165,** 155 (1990).